

## Synthesis of Nitrogen Doped Carbon Quantum Dots/Magnetite nanocomposites for efficient removal of methyl blue dye pollutant from contaminated Water

Aschalew Tadesse<sup>a, c</sup>, Dharmasoth Rama Devi<sup>b</sup>, Mabrahtu Hagos<sup>a, d</sup>, GangaRao Battu<sup>b</sup> and K. Basavaiah<sup>a\*</sup>

<sup>a</sup>Department of Inorganic and Analytical Chemistry, Andhra University, Visakhapatnam-530003, India,

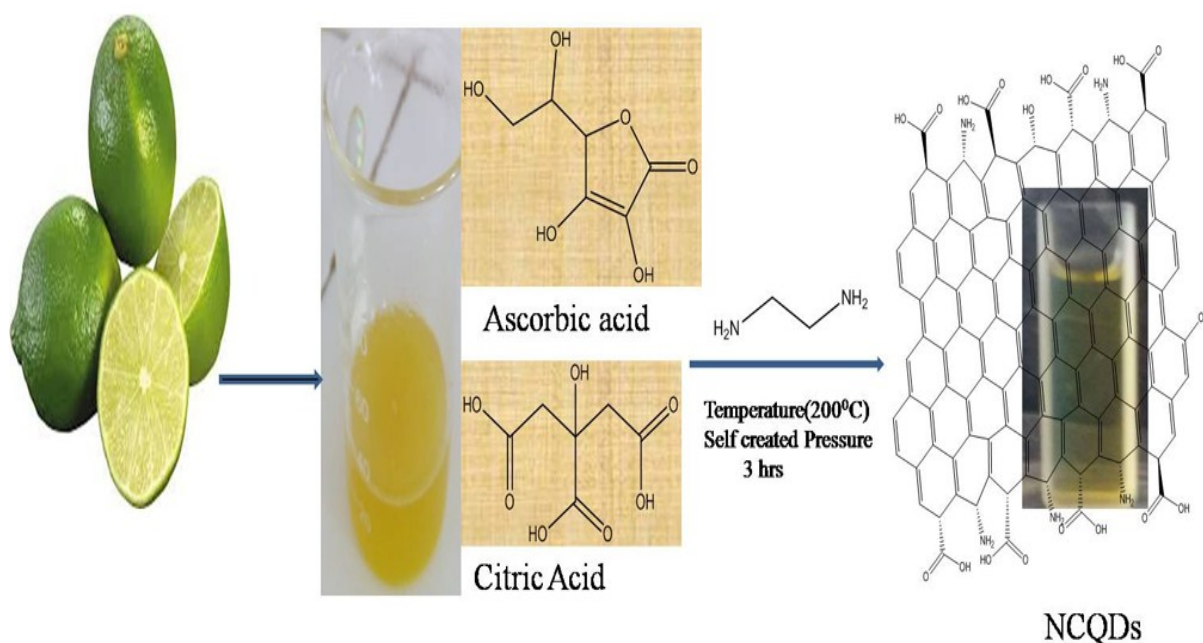
<sup>b</sup>AU College of Pharmaceutical Sciences, Andhra University, Visakhapatnam-530003, India

<sup>c</sup>Department of Applied Chemistry, Adama Science and Technology university, Adama-1888, Ethiopia

<sup>d</sup>Faculty of Natural and Computational Sciences, Woldia University, Woldia-400, Ethiopia

\*Corresponding Author Email: [klbasu@gmail.com](mailto:klbasu@gmail.com), Phone: +919908036203

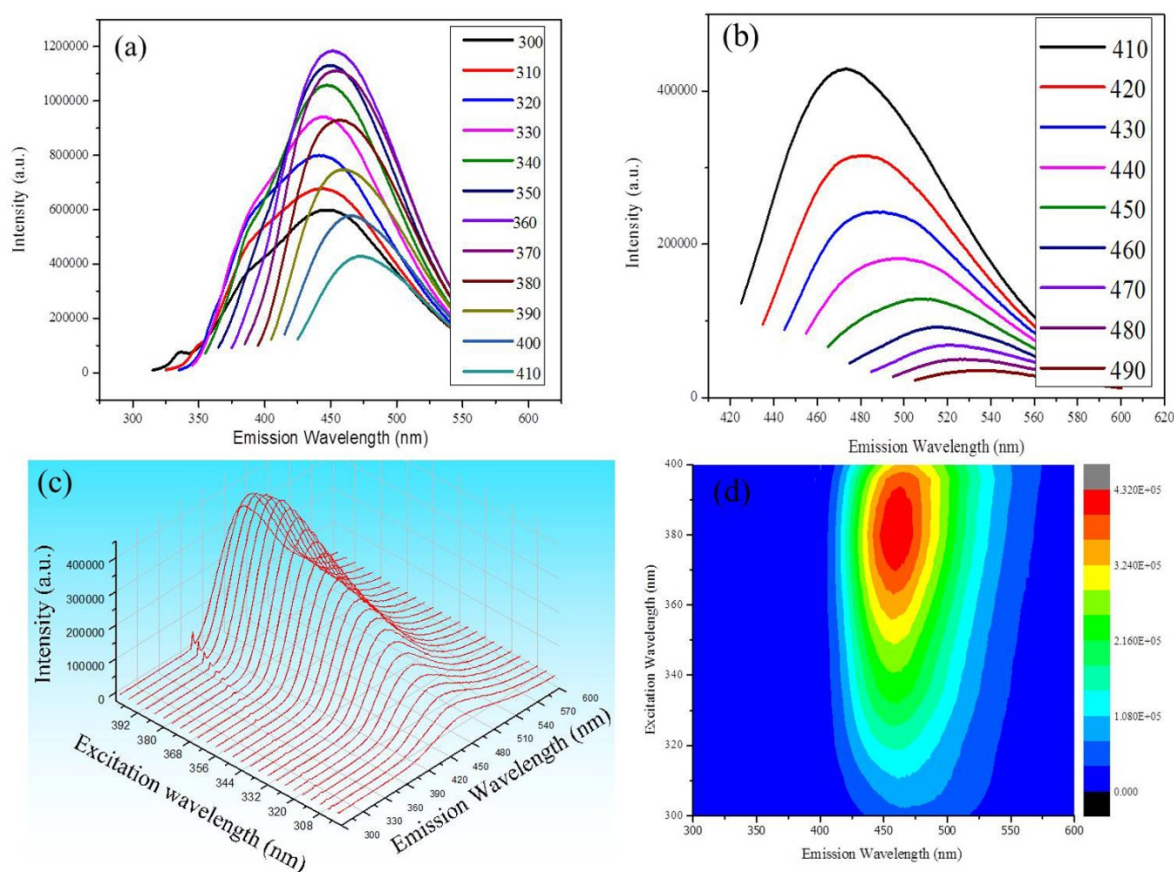
### Supplementary Information



**Fig. ESI1:** schematic representation of hydrothermal synthesis of NCQDs using lemon juice as precursor and ethylenediamine as coreagent

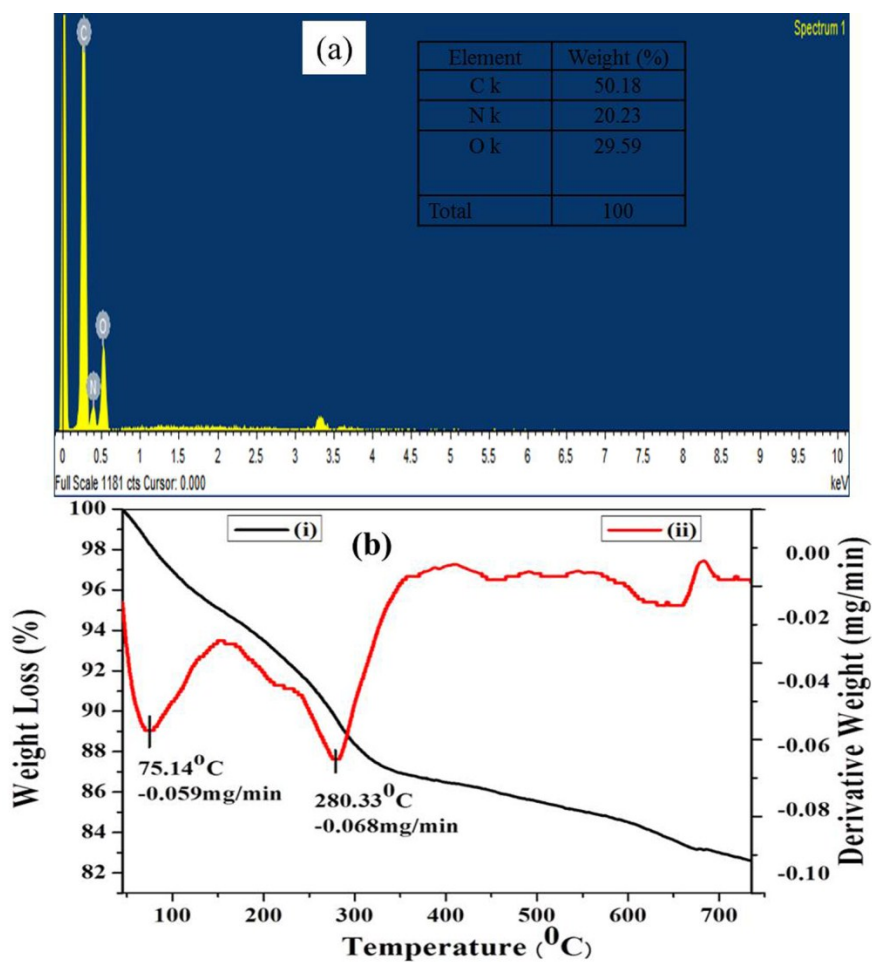
As seen from Fig.ESI2 (a and b), the sample shows strong fluorescence with symmetrical peaks. Emission intensity increases as excitation wavelength increase from 310 nm to 360 nm then start decreasing and maximum emission intensity obtained at excitation wavelength of 360 nm. Fig.ESI2(d) indicate excitation and emission contour map of NCQDs which showed

multicolour emission of NCQDs. The photoexcitation of nitrogen doped carbon quantum dots may be due to  $\pi$ -plasmon absorption in the core carbon nanoparticles<sup>1</sup> and to large extent photoluminescence significantly affected by the surface chemistry of the NCQDs.<sup>2</sup> The as synthesized NCQDs show high FL quantum yield (QY ~31%) relative to the standard Quinine sulphate.



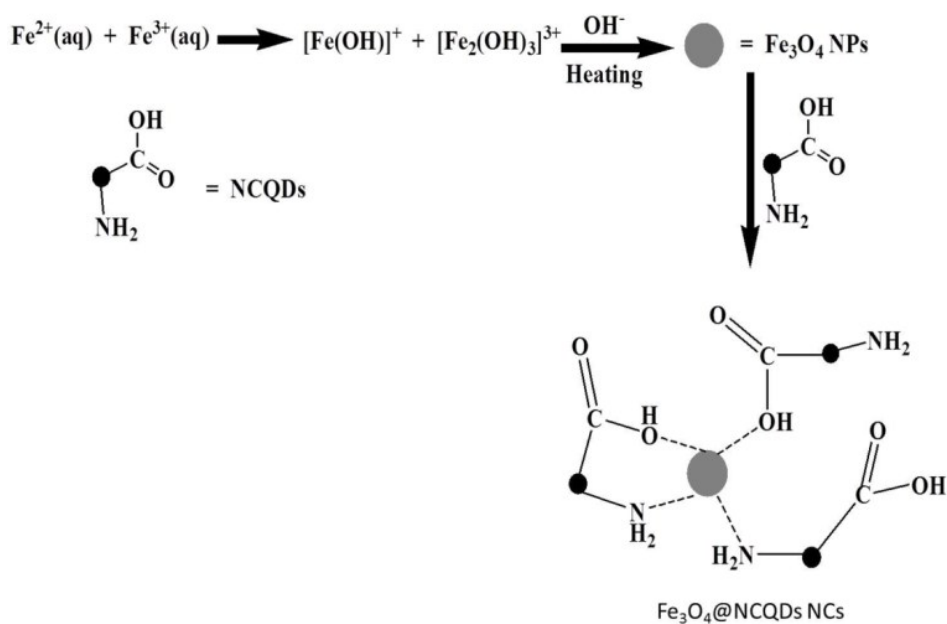
**Fig. ESI2** (a) Fluorescence emission spectra of NCQDs under excitation wavelength (300 to 410) (b) excitation wavelength (410 to 490) (c) 3D Fluorescence spectra of NCQDS (d) Excitation and emission contour map of NCQDs

Result from elemental composition analysis of EDX spectrum (Fig.ESI3a) reveal the presence of C, O and N in the as synthesized material indicating well formation of nitrogen doped carbon quantum dots.



**Fig. ESI3** (a) EDS spectra of NCQDs (b) ((i) Thermogravimetric analysis (TGA) and (ii) differential thermal analysis (DTA) of  $\text{Fe}_3\text{O}_4@\text{NCQDs}$  NCs

**Scheme ESI1** A plausible formation mechanism of  $\text{Fe}_3\text{O}_4@\text{NCQD}$  NCs



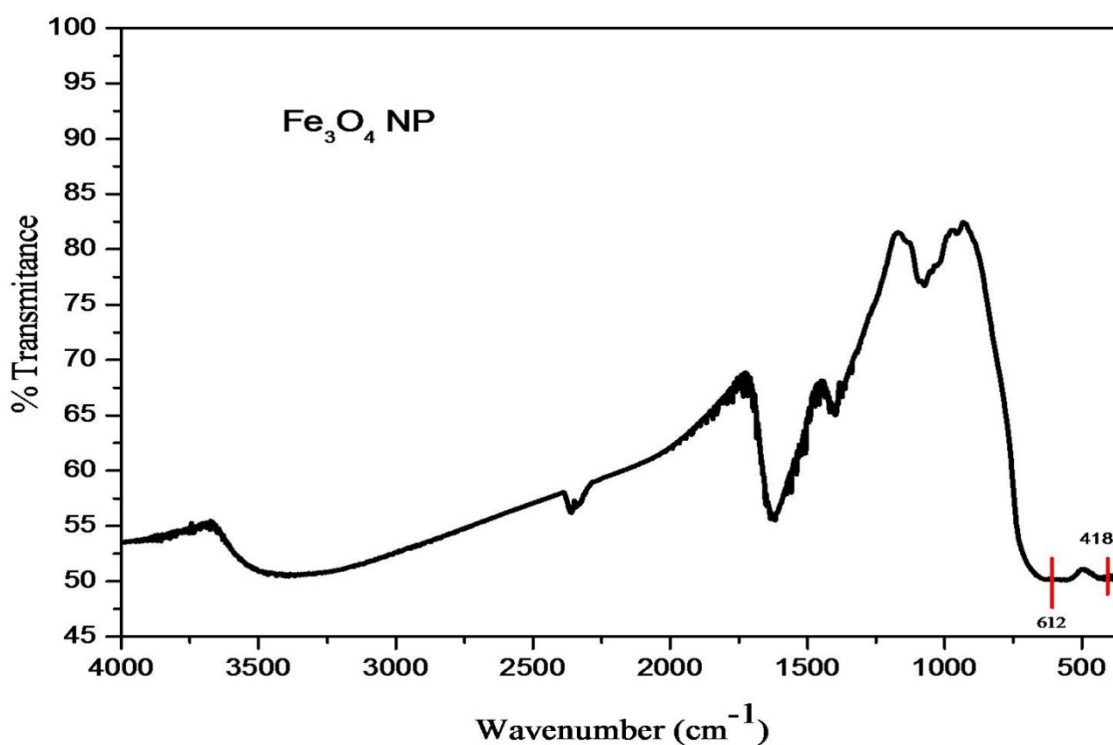


**Fig. ESI4** FTIR spectrum of Fe<sub>3</sub>O<sub>4</sub> NPs

As shown in Fig.3c, the TGA-DTA of Fe<sub>3</sub>O<sub>4</sub>@NCQDs NCs has three characteristic decomposition stages. Weight loss (~6.0 %) of Fe<sub>3</sub>O<sub>4</sub>@NCQDs NCs in the first stage was due to the loss of water, and weight loss (~13.6 %) in the second stage was due to the decomposition of the amine, hydroxyl and carbonyl groups on the surface of NCQDs in nanocomposites structure. In Fig.ESI3b(i), (DTA curve) three peaks were observed: peak between 39 and 150 °C with a maximum at 75.14 °C, peak between 150 and 405 °C with a maximum at 280.33 °C, and the third peak between 404 and 735 °C with a maximum at 650 °C which correspond to three stage transition of the Fe<sub>3</sub>O<sub>4</sub>@NCQDs NCs. The first stage transition could be due to the loss of water, while the second was due to decomposition of the amine, hydroxyl and carbonyl groups on the surface of carbon quantum dots and third attributed to the arrangement of the structure of the Fe<sub>3</sub>O<sub>4</sub>@NCQDs NCs.<sup>3</sup>

Magnetic property of material is one of the important properties which decide the easy separation of the materials after environmental remediation. The magnetic properties of the synthesised Fe<sub>3</sub>O<sub>4</sub>@NCQDs NCs have been investigated by studying the field dependence magnetization at room temperature using vibrating sample magnetometer (VSM) in the range of -15 kOe to 15 kOe applied magnetic field. Fig.ESI5 shows the M–H curves of Fe<sub>3</sub>O<sub>4</sub>@NCQDs NCs measured at 300 K and the forward and backward magnetization curves overlap completely.

Fig.ESI5 inset in up left side showed almost zero hysteresis loop in narrow range from -0.5 kOe to 0.5 kOe indicating their superparamagnetic behaviour.<sup>4</sup> The saturation magnetization ( $M_s$ ) value of  $\text{Fe}_3\text{O}_4@\text{NCQDs}$  NCs is  $24.6 \text{ emu/g}$ . The reduced  $M_s$  of the  $\text{Fe}_3\text{O}_4@\text{NCQDs}$  NCs in comparison to  $M_s$  of bulk magnetite is possibly due to the presence of non-magnetic NCQDs with the magnetic ordering of the iron oxide nanosystem.<sup>5</sup> In Fig.ESI5 inset right bottom showed the easy separation of  $\text{Fe}_3\text{O}_4@\text{NCQDs}$  NCs from solution by using external magnet.

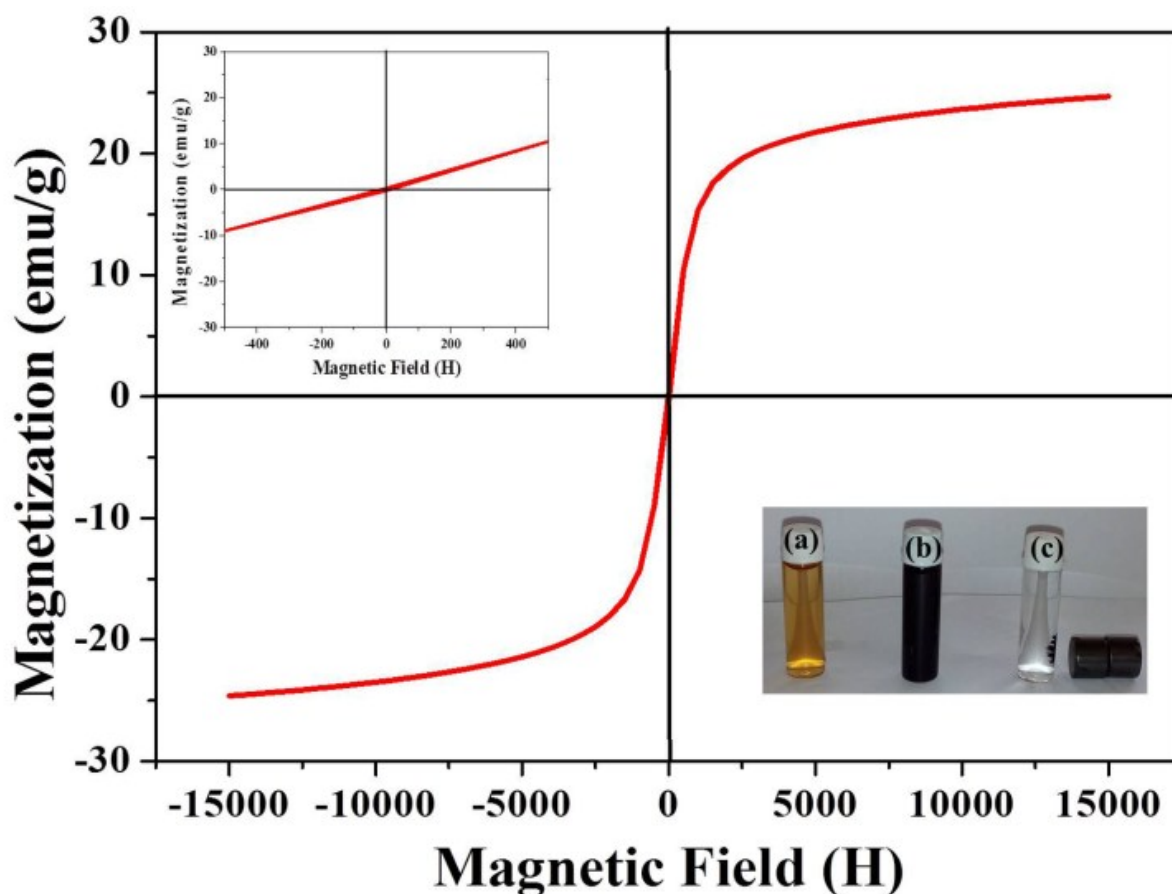


**Fig.ESI5** The room temperature magnetization curve of  $\text{Fe}_3\text{O}_4@\text{NCQDs}$  NCs (top up left side inset show hysteresis loop in narrow expanded scale range of -0.5 kOe to 0.5 kOe and bottom right side inset show easy separation of the  $\text{Fe}_3\text{O}_4@\text{NCQDs}$  NCs using external magnet (a) NCQDs solution (b) colloidal suspension and (c) separation of synthesised  $\text{Fe}_3\text{O}_4@\text{NCQs}$  NCs in presence of external magnet)

**Table ESI1:** Isotherm parameters for MB dye solution onto Fe<sub>3</sub>O<sub>4</sub>@NCQDs NCs

Temp. (K)	Langmuir				Freundlich			Temkin		
	Q <sub>o</sub> (mg/g)	b	R <sub>L</sub>	R <sup>2</sup>	K <sub>F</sub> (mg/g)	n	R <sup>2</sup>	A <sub>T</sub>	b <sub>T</sub> (J/mol)	R <sup>2</sup>
293	24.888	2.679	0.436	0.985	19.491	1.838	0.987	27.252	450.957	0.977
298	24.480	2.157	0.428	0.989	17.069	1.842	0.993	22.265	469.384	0.974
303	24.414	1.834	0.414	0.946	16.317	1.811	0.997	19.357	477.986	0.944

**Table ESI2 :** Thermodynamic Parameters of MB dye adsorption onto Fe<sub>3</sub>O<sub>4</sub>@NCQDs nanocomposites

Temperature(K)	ΔG <sup>0</sup> (KJ/mol)	ΔH <sup>0</sup> (KJ/mol)	ΔS <sup>0</sup> (KJ/mol)
293	-8.208	-38.591	-0.104
298	-7.677		
303	-7.203		

**Table ESI3:** Kinetic Parameters for adsorption of MB onto Fe<sub>3</sub>O<sub>4</sub>@NCQDs nanocomposites

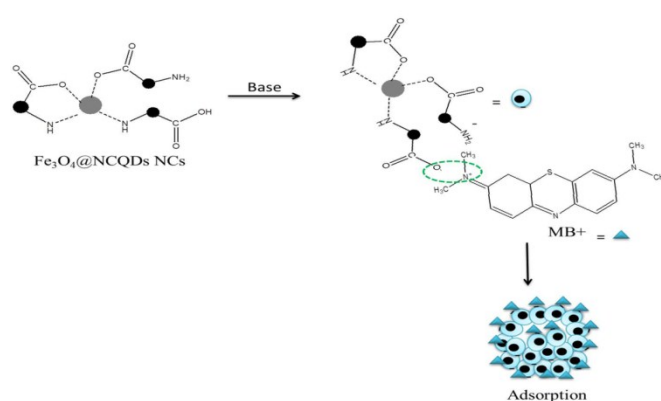
Pseudo –first order			Pseudo-second order			
K <sub>1</sub> (min <sup>-1</sup> )	Q <sub>e</sub> (calc.)	R <sup>2</sup>	K <sup>2</sup>	Q <sub>e</sub> (calc.)	h	R <sup>2</sup>
0.228	3.125	0.939	0.194	14.14	38.91	0.999

**Table ESI4:** Comparison of adsorption capacity of nanocomposites for removal of methylene blue from aqueous solution

Nanocomposites	Maximum adsorption capacity q <sub>m</sub> (mg g <sup>-1</sup> )	References
Poly(3,4-propylenedioxythiophene)/ MnO <sub>2</sub> composites	13.94	6
Magnetic graphene/calcium alginate (G-Fe <sub>3</sub> O <sub>4</sub> /CA)	17.27 at 20 °C	7
CS/Fe <sub>3</sub> O <sub>4</sub> /GO	30.01	8
OMWCNT-Fe <sub>3</sub> O <sub>4</sub>	41.50	9
Magnetic multi-wall carbon nanotube (Fe <sub>3</sub> O <sub>4</sub> -MWCNT)	15.74	10
Graphenenanosheet/magnetite (GNS/Fe <sub>3</sub> O <sub>4</sub> ) composite	43.82	11
Fe <sub>3</sub> O <sub>4</sub> @NCQDs	24.5 at 20 °C	This work

Adsorption mechanism of dye on to the surface of  $\text{Fe}_3\text{O}_4@\text{NCQDs}$  NCs is based on electrostatic interaction between negatively charged  $\text{Fe}_3\text{O}_4@\text{NCQDs}$  NCs surfaces and cationic dyes. In basic media, the carboxyl surface functional group of the NCs become negatively charged while MB dyes become positively charged on nitrogen in the structure. These oppositely charged species attract each other through electrostatic interaction and form coordinate covalent bond and hence MB dye adsorbed on to the surface of  $\text{Fe}_3\text{O}_4@\text{NCQDs}$  NCs. In addition to electrostatic interaction, MB dye may also entrapped in hole space available in collected nanocomposites.

**Scheme 2** Possible adsorption mechanism for adsorption of MB dye on to  $\text{Fe}_3\text{O}_4@\text{NCQDs}$  NCs



## References

1. K. A. S. Fernando, S. Sahu, Y. Liu, W. K. Lewis, E. A. Guliyants, A. Jafariyan, P. Wang, C. E. Bunker and Y.-P. Sun, *ACS Appl. Mater. Interfaces*, 2015, 7, 8363–8376.
2. S. N. Baker and G. A. Baker, *Angew. Chem. Int. Ed Engl.*, 2010, 49, 6726–6744
3. E. Mansfield, in *Modeling, Characterization, and Production of Nanomaterials*, 2015, pp. 167–178.
4. M. Mahdavi, F. Namvar, M. Ahmad and R. Mohamad, *Molecules*, 2013, 18, 5954–5964.
5. K. Bhattacharya and P. Deb, *Dalton Trans.*, 2015, 44, 9221–9229.
6. R. Jamal, L. Zhang, M. Wang, Q. Zhao and T. Abdiryim, *Materials International*. 26 (2016) 32–40.
7. N. Song, X.-L. Wu, S. Zhong, H. Lin and J.-R. Chen, *J. Mol. Liq.* 212 (2015) 63–69.
8. H. V. Tran, L. T. Bui, T. T. Dinh, D. H. Le, C. D. Huynh and A. X. Trinh, *Materials Research Express*. 4 (2017) 035701.
9. O. Duman, S. Tunç, T. G. Polat and B. K. Bozoğlan, *Carbohydr. Polym.* 147 (2016) 79–88.
10. J.-L. Gong, B. Wang, G.-M. Zeng, C.-P. Yang, C.-G. Niu, Q.-Y. Niu, W.-J. Zhou and Y. Liang, *J. Hazard. Mater.* 164 (2009) 1517–1522.
11. L. Ai, C. Zhang and Z. Chen, *J. Hazard. Mater.* 192 (2011) 1515–1524.